On the dependence of the efficiency of a 240 GHz high-power gyrotron on the displacement of the electron beam and on the azimuthal index

O. Dumbrajs,[1] K. A. Avramidis,[2] J. Franck,[2] and J. Jelonnek[2]
[1]*Institute of Solid State Physics (ISSP), Association EUROATOM-University of Latvia, Kengaraga iela 8, LV-1063 Riga, Latvia*
[2]*Karlsruhe Institute of Technology (KIT), Institute for Pulsed Power and Microwave Technology (IHM), Association EURATOM-KIT, Kaiserstrasse 12, 76131 Karlsruhe, Germany*

(Received 29 November 2013; accepted 5 January 2014; published online 15 January 2014)

Two issues in the cavity design for a Megawatt-class, 240 GHz gyrotron are addressed. Those are first, the effect of a misaligned electron beam on the gyrotron efficiency and second, a possible azimuthal instability of the gyrotron. The aforementioned effects are important for any gyrotron operation, but could be more critical in the operation of Megawatt-class gyrotrons at frequencies above 200 GHz, which will be the anticipated requirement of DEMO. The target is to provide some basic trends to be considered during the refinement and optimization of the design. Self-consistent calculations are the base for simulations wherever possible. However, in cases for which self-consistent models were not available, fixed-field results are presented. In those cases, the conservative nature of the results should be kept in mind. © *2014 AIP Publishing LLC*. [http://dx.doi.org/10.1063/1.4862446]

I. INTRODUCTION

DEMO is intended to be the first electricity producing fusion power plant following ITER. Electron cyclotron heating and current drive (ECRH&CD) are expected to be the dominant heating and current drive systems. According to Ref. 1, optimum efficiencies of ECRH&CD are found for frequencies around 230 GHz and 290 GHz for the steady-state and the pulsed DEMO. High-power, continuous-wave (CW) gyrotron operation at such frequencies requires a very high-order operating mode to keep the ohmic loading of the walls within acceptable limits. In Ref. 2, a preliminary design of a conventional hollow-cavity resonator capable of generating about 1.3 MW of power at 238 GHz is discussed. The proposed operating mode is $TE_{50,17}$ (eigenvalue ∼ 119). It is known that, compared to hollow-cavity, the coaxial-cavity resonator is capable of supporting single-mode operation at even higher-order modes.[3] For this reason, KIT is expanding its research on coaxial-cavity gyrotrons towards frequencies above 200 GHz, starting gyrotron research for a frequency step-tunable, coaxial-cavity type gyrotron at around 240 GHz.[4] Targeting at 2 MW of output power, or, alternatively, at highly reliable operation at 1.5 MW, the operating $TE_{49,29}$ mode (eigenvalue ∼ 158) is currently considered to be appropriate. In a preliminary cavity design, already obtained, the $TE_{49,29}$ mode ensures stable single-mode operation suppressing mode competition.

In this paper, two issues will be addressed, which, for such a high-order mode, have not been considered in other publications: (i) The effect of a misaligned (i.e., shifted and/or tilted) electron beam on the gyrotron efficiency and (ii) a possible azimuthal instability of the gyrotron. The studies are motivated by the fact that the aforementioned effects could be critical in high-power gyrotrons in the 200–300 GHz frequency range, considering the short wavelength and the very high-order operating mode. To illustrate the latter point further, it should be noted that the operating $TE_{34,19}$ mode of the 170 MW, 2 MW pre-prototype coaxial gyrotron at KIT[5] has an eigenvalue of ∼105 already. To the authors' knowledge, this operating mode is so far the highest-order mode, for which robust excitation has been experimentally demonstrated in a gyrotron. The studies presented in this paper will focus on a preliminary 240 GHz coaxial cavity design. However, the conclusions can be of more general importance regarding gyrotron designs at this frequency and power range.

Table I shows the basic operating parameters of the gyrotron design under study. A beam current of 55 A, which is compatible with the present electron gun technology, can yield a generated power of ∼1.5 MW CW. However, with a current of 75 A, which can be achieved with advanced electron gun technologies, already underway,[6] the gyrotron can yield 2.1 MW of generated power. Because of the employed very high-order $TE_{49,29}$ mode, the ohmic wall loading constraint is satisfied in any case (i.e., it is kept below 2 kW/cm^2).

The resonator outer wall radius is shown in Fig. 1.

The axial profile of RF field in this cavity is shown in Fig. 2.

In the fixed-field, cold cavity approximation and for a beam current of 55 A, one finds an operating frequency of $f = 239.925\,GHz$, a diffraction quality factor of $Q_{diff} = 1838$, and an output power of $P_{out} = 1.2\,MW$, yielded at the efficiencies $\eta_{\perp} = 48\%$, $\eta_{tot} = 29\%$. Self-consistent calculations using the code COAXIAL[7] provide the following results: $f = 239.874GHz$, $Q_{diff} = 2139$, $P_{out} = 1.4\,MW$, $\eta_{\perp} = 55\%$, and $\eta_{tot} = 33\%$, whereas self-consistent calculations using the more advanced code-package EURIDICE[8] result in $f = 239.939GHz$, $Q_{diff} = 2720$, $P_{out} = 1.5\,MW$, $\eta_{\perp} = 58\%$, and $\eta_{tot} = 36\%$. The discrepancies between the fixed-field and the self-consistent results are well known for low-Q gyrotrons. Also, it is a fact that the fixed-field results are usually conservative results. For this reason, self-consistent

TABLE I. Operating parameters.

Central frequency	240 GHz
Magnetic field	9.53 T
Beam voltage	76 kV
Beam current	55 A/75 A
Beam radius	10 mm
Electron beam pitch factor	1.3

calculations are the base for simulations, wherever possible. However, in those cases for which self-consistent models are not available (e.g., tilted electron beam), fixed-field results are presented. In those cases, the conservative nature of the results should be kept in mind.

II. EFFECT OF ELECTRON BEAM MISALIGNMENT ON THE GYROTRON EFFICIENCY

The ordinary theory describing the interaction between gyrating electrons and the RF field in gyrotrons assumes axial symmetry, which greatly simplifies the treatment of the problem. In practice, however, a misalignment between the electron-optical system of a gyrotron and the magnetic field axis with respect to the center axis of the gyrotron is very likely during production (see Ref. 9 and references therein). Moreover, it is intuitively clear that the significance of those misalignments increases with decreasing wavelength. The wavelength of a 240 GHz gyrotron ($\lambda = 1.25\,mm$) is about 30% shorter than the wavelength of the 170 GHz ITER gyrotron ($\lambda = 1.76\,mm$). In this paper, we use the fixed-field theory of electron beam misalignments developed in Ref. 9 to analyze the 240 GHz gyrotron design. Wherever possible, results obtained with the self-consistent approach are also presented.

In the case of a displacement of the electron beam axis with respect to the center of the cavity, the coordinates of the electron guiding centers in the resonator frame (R_b, ψ) and in the beam frame (R_0, ψ_0) are related as follows:

$$R_0^2 = R_b^2 - 2dR_b\cos\psi + d^2, \tag{1}$$

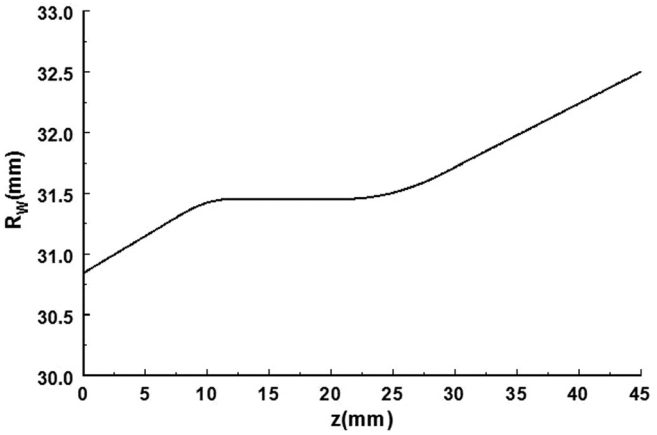

FIG. 1. Axial profile of the resonator wall radius in the 240 GHz gyrotron design.

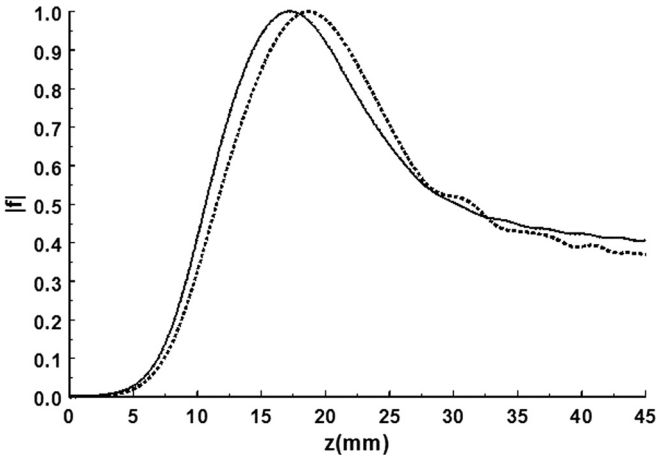

FIG. 2. The simulated axial profile of the transverse electric RF field in the cavity: Cold cavity approximation (solid) and self-consistent (dashed).

where d is defined as the distance between the center axis and the beam axis. In the case of a beam displacement parallel to the cavity axis (i.e., beam shift), the distance d is constant. Instead, in the case of a tilt, the distance d varies along the z-axis in accordance with

$$d = \sqrt{(x_{00} + z\tan\alpha_x)^2 + (y_{00} + z\tan\alpha_y)^2}. \tag{2}$$

In (2), x_{00} and y_{00} are transverse coordinates of the beam frame origin with respect to the origin of the resonator frame at the entrance ($z = 0$), and the angles $\alpha_{x,y}$ are the tilt angles in corresponding directions. Since the x-axis and y-axis can be chosen arbitrarily, without loss of generality, one can assume that the beam is tilted in $x-$direction only.

The effect of the beam shift on the interaction efficiency of the gyrotron is illustrated by the results presented in Figure 3 and in Table II. In Figure 3, the contours of equal efficiencies are shown, calculated with the cold-cavity, fixed-field approximation. Table II shows the results which have been obtained by self-consistent simulations using the

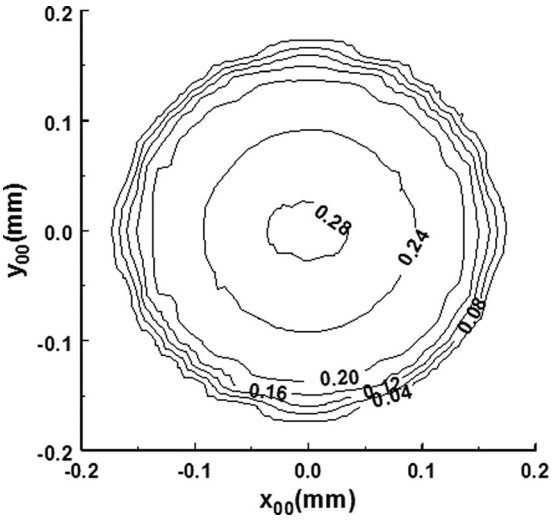

FIG. 3. Fixed-field results for a parallel displacement of the electron beam (i.e., shift only, no tilt): The interaction efficiency η_{tot} is plotted as a function of the transverse coordinates. An ideal electron beam with a radius of 10 mm is assumed.

TABLE II. Self-consistent results for electron beam parallel displacement.

Beam shift (mm)	Electron efficiency (%)
0.00	37.1
0.10	37.1
0.20	36.5
0.25	36.0
0.27	35.3
0.28	Mode loss

EURIDICE code package. The beam shift in EURIDICE is treated in the same manner as in Ref. 10. In both cases, single-mode calculations with an ideal electron beam (i. e., assuming no spread in guiding-center, energy, and velocity) have been performed.

According to the fixed-field model (Fig. 3), a shift of the order of $d = 0.15$ mm leads to mode loss. However, in the self-consistent approach, the necessary shift for mode loss is $d = 0.28$ mm (see Table II). Note that in the fixed-field approach, the corresponding shift for mode loss for a 170 GHz 1 MW hollow-cavity gyrotron is 0.60 mm,[9] whereas highly realistic self-consistent simulations of a 170 GHz, 2 MW coaxial gyrotron (including beam shift, spreads in electron energy, velocity, and guiding-center, as well as mode competition and realistic magnetic field profile) showed that the shift necessary for mode loss is 0.80 mm.[11] From these results, we could suggest that although the wavelength is reduced by only 30% from 170 GHz to 240 GHz, the corresponding tolerance in beam shift decreases by ~70%.

Figure 4 shows the gyrotron efficiency as a function of the tilt angle of the electron beam. The fixed-field approach of Ref. 9 was used to perform the single-mode calculations, assuming no spread in the beam parameters. In the fixed-field calculation, a tilt angle of 0.6° leads to a mode-loss.

Finally, the combined effect of electron beam displacement and tilt was also addressed in a similar fashion. The results are shown in Fig. 5 for a tilt equal to 0.5° (a) and 1° (b).

It is interesting that in the fixed-field calculations, the deteriorating effect of the tilt on the gyrotron efficiency (Fig. 4) can be mitigated by a corresponding shift of the beam at the entrance (Fig. 5) if such a shift results, on average, in a better matching of the beam and resonator axes in the interaction space. By considering displacement-tilt value pairs for constant efficiency (see Table III), it is possible to roughly estimate which "displacement" compensates which "tilt angle" (and vice versa). The tilt θ can be interpreted as a beam shift d in the x_{00}-y_{00} (entrance) plane, with the beam axis fixed at (0,0) at a certain height h over the x_{00}-y_{00} plane according to $h = d/\tan(\theta)$. Since the considered tilt angles are

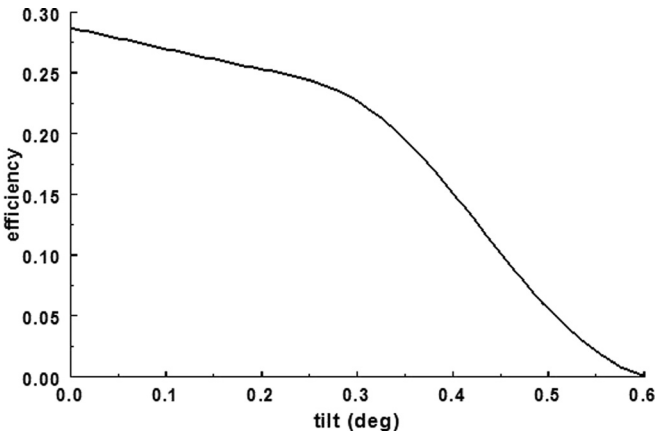

FIG. 4. Fixed-field results for electron beam tilt: Efficiency as a function of the tilt angle.

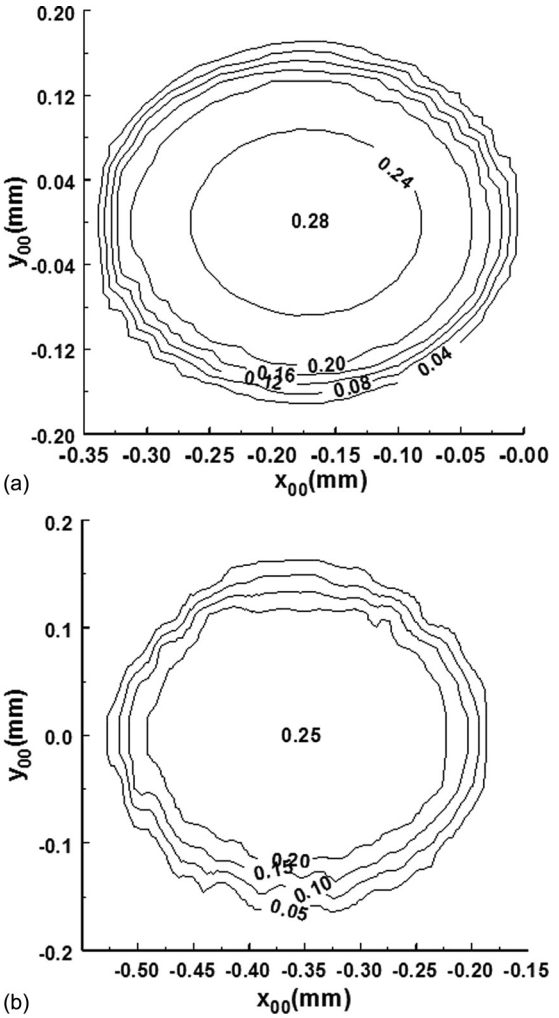

FIG. 5. Fixed-field results for electron beam shift and tilt: Efficiency as a function of transverse coordinates for (a) a tilt angle 0.5° and (b) a tilt angle 1°. The electron beam radius is 10 mm.

TABLE III. Displacement-tilt pairs at constant efficiencies.

Efficiency	Pairs
0.28	(0.00 mm; 0.00°), see Figs. 3–5(a)
	(0.18 mm; 0.50°), see Fig. 5(a)
	Slope: 0.36 mm/deg
0.24	(0.00 mm; 0.26°), see Fig. 4
	(0.08 mm; 0.50°), see Fig. 5(a)
	Slope: 0.33 mm/deg
	(0.09 mm; 0.00°), see Fig. 3
	(0.27 mm; 0.50°), see Fig. 5(a)
	Slope: 0.36 mm/deg

small, the approximation $\theta \approx \tan(\theta)$ is valid. If d equals the defined beam displacement, $h(x_{00},\theta)$ is the z-coordinate where the beam axis crosses the z-axis. If the interaction efficiency is mainly dependent on the closeness of h and the field maximum (see Fig. 2), lines of constant efficiency $\eta(x_{00},\theta)$ should all have the same slope $\Delta x_{00}/\Delta\theta$.

The slopes of the 28%-efficiency line and of the two extremal 24%-efficiency lines lie between 0.33 mm/degree and 0.36 mm/degree, or 19 mm and 21 mm. This is quite accurately the z-coordinate of the field maximum, which is expected to be the main interaction point.

The results presented in the Figures 3–5 are obtained assuming that there is no spread in the electron guiding center radii. However, in practice, the spread is always present. In Figures 6–8, the effect of the shift and tilt on the interaction efficiency is shown, assuming that there is a spread in the guiding-center of $2\lambda/5$: $R_b = 10 \pm 0.25$ mm.

Apparently, a guiding-center spread as large as 0.5 mm deteriorates the efficiency only slightly, by only ~15%. Since it is expected that, by proper emitter design, this spread will be smaller by a factor of 2 in the 240 GHz gyrotron and that there is a monotonic dependence between spread and beam shift/tilt on the gyrotron efficiency, the finite width of the electron beam does not seem to be an important issue.

III. REGIONS OF AZIMUTHAL INSTABILITY

At present, MW-class millimeter-wave, CW gyrotrons operate at high-order modes, hence in the region of a very dense spectrum of eigenmodes. Therefore, in studying the interaction of an electron beam with the eigenmodes of the gyrotron cavity and in parallel with representing the electromagnetic (EM) field as a superposition of a number of discrete eigenmodes, the wave envelope representation can be used as well.[12] As the gyrotron resonator is open in its axial direction (direction of the external magnetic field), the axial structure of the EM field is influenced by the electron beam. Therefore, in the case of a wave envelope representation of the EM field, this envelope in non-stationary regimes depends on time and axial and azimuthal coordinates.

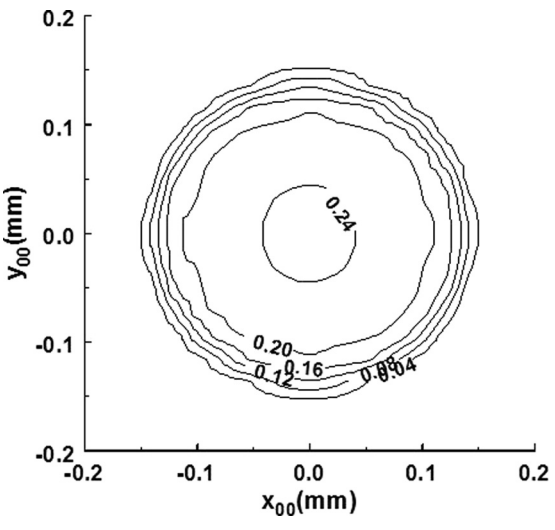

FIG. 6. Same as Fig. 3, but $R_b = 10 \pm 0.25$ mm.

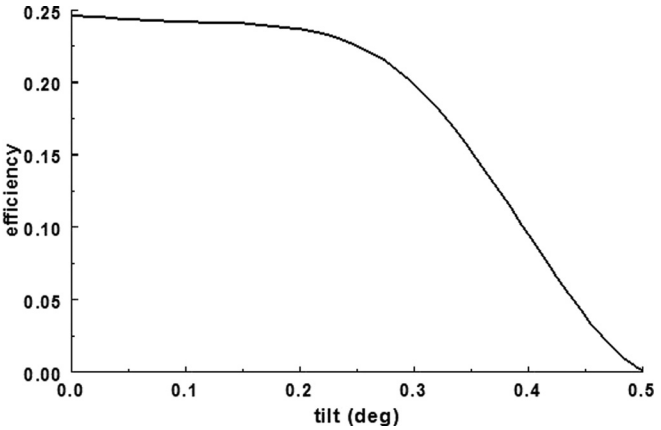

FIG. 7. Same as Fig. 4, but $R_b = 10 \pm 0.25$ mm.

Correspondingly, the EM field can be represented as an azimuthally rotating wave envelope $E \propto f(z,t,\varphi)\exp\{-i(\omega_0 t - m_0\varphi)\}$ (here, ω_0 and m_0 are the carrier frequency and carrier azimuthal index, respectively).

A gyrotron operation with the EM field represented as an azimuthally rotating wave envelope was first studied in Ref. 9. In Ref. 9, it was found that oscillations in a gyrotron with parameters optimal for the maximum efficiency become unstable when the normalized parameter $W = \pi\beta_{\perp 0}^2 m_0$, characterizing the azimuthal index of the operating mode, exceeds a certain threshold value of about 25. (Here, $\beta_{\perp 0}$ is the initial orbital electron velocity normalized to the speed of light.) Then, in Refs. 13 and 14, a more detailed analysis of the spatio-temporal chaos occurring in some regimes was carried out, and the regions of stable operation were distinguished from the regions of automodulation, and those, in turn, from chaotic oscillations. This work was continued in Refs. 15 and 16 where the regions of stable operation in the gyrotron parameter space were determined. It was shown that the discrepancy between the theory based on the cold-cavity approximation of all competing modes and the self-consistent theory can be explained by the fact that the axial structures of modes composing the wave envelope become different due to the electron beam. It was also found in Ref. 15 that at low currents, the dependence of the gyrotron efficiency on the azimuthal parameter, $W = \pi\beta_{\perp 0}^2 m_0$, can have a sawtooth shape.

The self-consistent set of equations includes the equation for electron motion, the equation for the wave envelope, and corresponding boundary and initial conditions. The equation for electron motion, i.e., for the normalized orbital momentum of electrons, in the case of the fundamental cyclotron resonance, has the standard form

$$\frac{dp}{d\varsigma} + i(\Delta + |p|^2 - 1)p = if(\varsigma,\tau,w). \tag{3}$$

Here, p is the complex orbital electron momentum normalized to its initial value, $\Delta = (2/\beta_{\perp 0}^2)[1 - (\Omega_0/\omega)]$ is the cyclotron resonance mismatch between electron cyclotron frequency at the entrance Ω_0 and the wave carrier frequency ω, $\varsigma = (\beta_{\perp 0}^2/2\beta_{z0})(\omega z/c)$ is the normalized axial coordinate, and f is the dimensionless wave envelope. Below, we will

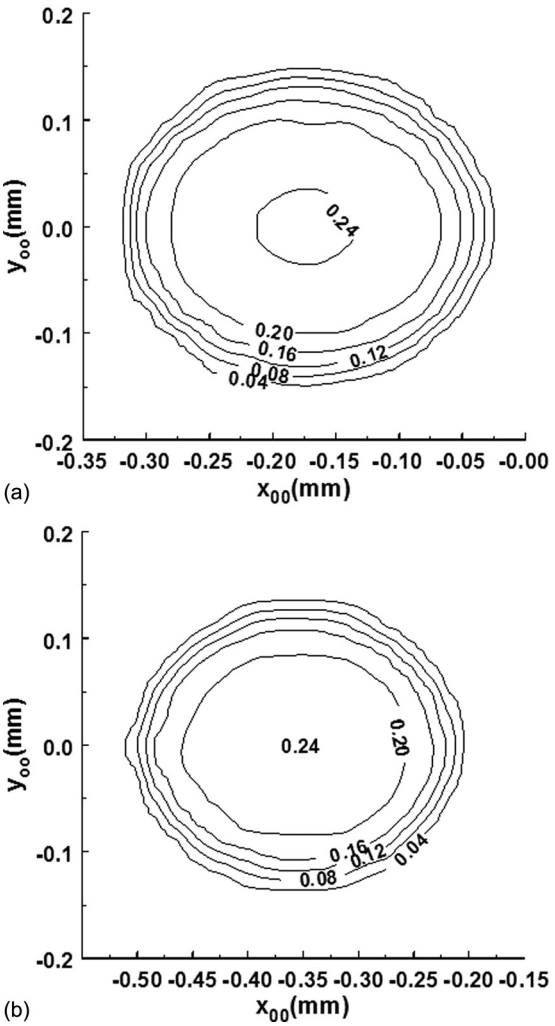

FIG. 8. Same as Fig. 5, but $R_b = 10 \pm 0.25$ mm.

analyze the quasi-stationary case, in which the electron transit time via the interaction space is much shorter than the time of wave envelope evolution $T = L/v_z \ll |f|/|\partial f/\partial t|$; here, the term on the right-hand side is of the order of the cavity filling time Q/ω. As follows from our presentation of the wave envelope above, we assume that this envelope depends on three variables. Correspondingly, its evolution is described by the partial differential equation

$$\frac{\partial^2 f}{\partial \varsigma^2} - i\frac{\partial f}{\partial \tau} - i\frac{\partial f}{\partial w} = \frac{I}{2\pi}\int_0^{2\pi} p\, d\vartheta_0. \tag{4}$$

The second derivative of this envelope on the axial coordinate in (4) follows from the fact that the gyrotron operates at frequencies near cutoff. In (4), $\tau = \left(\beta_{\perp 0}^4/8\beta_{z0}^2\right)\omega_0 t$ is the dimensionless time and $w = \left(\beta_{\perp 0}^2/2\right)m_0\varphi$ is the normalized azimuthal coordinate. In Eqs. (3) and (4), $0 \le \varsigma \le \varsigma_{out}$.

The boundary conditions for (3) and (4) are discussed in Ref. 15. In what follows we assume that at the entrance the electrons are uniformly distributed over initial gyrophases ϑ_0. For our study, it is important to present here the initial condition for the wave envelope

$$f(\tau = 0) = \left[a + b\sin\left(2\pi\frac{w}{W}\right)\right]\sin\left(\pi\frac{\varsigma}{\varsigma_{out}}\right). \tag{5}$$

In (5), the parameter a defines the initial amplitude of the envelope, while the parameter b characterizes the initial azimuthal nonuniformity of this envelope. Results presented below were obtained for $a = 0.1$ and $b = 0.01$. The dependence of the results on these parameters, i.e., on the initial azimuthal nonuniformity of the electron emission, was studied in Ref. 15.

Dependencies of the gyrotron orbital efficiency $\eta_\perp$ averaged over all electron beamlets with different azimuthal coordinates are shown in Fig. 9. For these results, the normalized interaction length

$$\varsigma_{out} = \pi\left(\beta_{\perp 0}^2/\beta_{z0}\right)(L/\lambda) \tag{6}$$

was chosen to be $\varsigma_{out} = 25.5$ (this length sometimes is called μ). The reasoning behind this choice is the following: The normalized interaction length ς_{out} contains the interaction length L, which usually is assumed to be the Gaussian width of the field profile. From the field profile shape in Fig. 2, we can assume that $L = 20$ mm, which leads to the chosen value $\varsigma_{out} = 25.5$.

According to Fig. 9, we can deduce that for beam currents of 55 A or 65 A, the 240 GHz gyrotron design exhibits very high efficiency, i.e., its operation is not prone to azimuthal instabilities. Problems could appear for lower beam current (45 A), and this has to be kept in mind. However, as shown in Table I, the planned nominal operation will involve a current of 55 A or higher.

It should be noted that the normalized interaction length (6) cannot be defined unambiguously for realistic cases because there is no rigorous definition of the interaction length L in the case of the usual, non-Gaussian field profile of Fig. 2. Consequently, only estimations of L can be used. The estimation used for the calculations of Fig. 9 is the most evident, in our opinion. However, we should notice that a different estimation could lead to very different results. For example, if we select $L = 14$ mm, which corresponds to the length of the

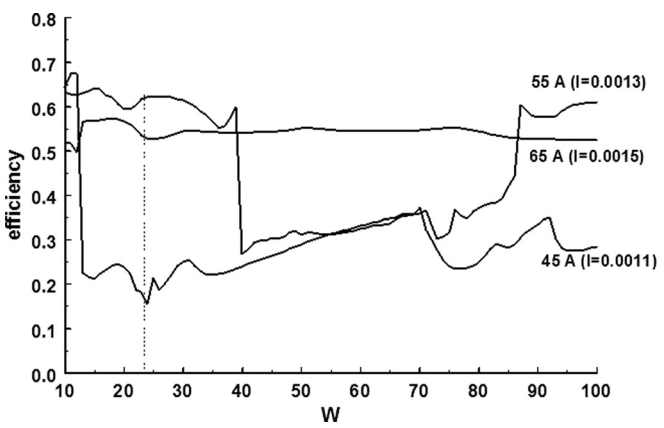

FIG. 9. Dependence of the gyrotron orbital efficiency $\eta_\perp$ averaged over the number of beamlets on the azimuthal parameter W for several values of the beam current parameter I. Here $\varsigma_{out} = 25.5$ and $\Delta = 0.42\,(B = 9.53T)$. Vertical dashed line shows the position of $W = 23.4$, which corresponds to the 240 GHz gyrotron operating parameters.

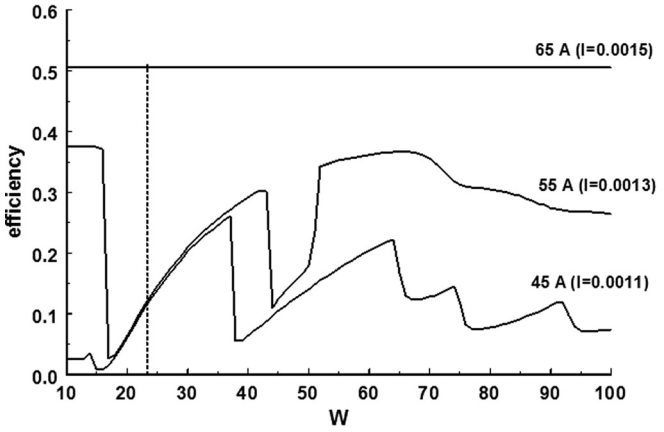

FIG. 10. Same as Fig. 9, but for $\varsigma_{out} = 17.7$.

straight section of the cavity (Fig. 1), we obtain $\varsigma_{out} = 17.7$. Then the results, shown in Fig. 10, indicate that at low currents 55 A and 45 A the dependence of the gyrotron efficiency on the azimuthal parameter W has a sawtooth shape, which leads to reduced efficiency for the 240 GHz design due to azimuthal instability. To avoid this and to achieve highly efficient operation, a current of 65 A should be used.

From the results above, it is clear that there is a possibility of azimuthal instability in the 240 GHz gyrotron design. However, a proper selection of the beam current can always remedy this. Given the uncertainties in the definition of L, a more extensive separate study is needed to reach more specific conclusions.

IV. SUMMARY

The single-mode fixed-field approximation has been used to examine the influence of a shifted and tilted electron beam on the gyrotron efficiency. In particular, it has been applied to an initial design for a MW-class, 240 GHz gyrotron. The fixed-field approximation has been compared with some results from self-consistent simulation. Based on these assumptions, it has been found out that, in comparison to existing MW-class gyrotrons and gyrotron designs at 170 GHz, the tolerances in tilt and shift decrease by a factor of more than 2, despite the fact that the wavelength is only 30% smaller. At the same time, it was seen that the degradation caused by the tilting can be mitigated by a corresponding shifting of the beam axis. Contrary to the shift and tilt, it was seen that even an extreme guiding-centre spread in the electron beam does not have a significant effect on the efficiency.

Based on the theory of wave envelope representation of the EM-field in the gyrotron cavity, the regions of stable gyrotron operation without azimuthal instability were also identified for two values of the normalized length of the interaction space. The trend is that these regions can be reached if the operating current of the gyrotron is increased. However, since it is not straightforward for the moment how to define the interaction length rigorously, this issue deserves a separate study.

ACKNOWLEDGMENTS

The work of O.D. was supported by the Latvian Grant No. 237/2012. The work of K.A.A, J.F., and J.J. was supported by the European Communities under the contract of Association between EURATOM and KIT and was carried out within the framework of the European Fusion Development Agreement. The views and opinions expressed herein do not necessarily reflect those of the European Commission.

[1]E. Poli, G. Tardini, H. Zohm, E. Fable, D. Farina, L. Figini, N. B. Marushchenko, and L. Porte, Nucl. Fusion **53**, 013011 (2013).
[2]M. V. Kartikeyan, J. Jelonnek, and M. Thumm, in *38th International Conference of Infrared Millimeter THz Waves, Mainz on the Rhine, Germany*, 1–6 September 2013, THP3-14.
[3]O. Dumbrajs and G. S. Nusinovich, IEEE Trans. Plasma Sci. **32**(3), 934–946 (2004).
[4]J. Jelonnek, K. Avramidis, J. Franck, G. Gantenbein, K. Hesch, S. Illy, J. Jin, A. Malygin, I. Pagonakis, T. Rzesnicki, A. Samartsev, T. Scherer, A. Schlaich, M. Schmid, D. Strauss, M. Thumm, and J. Zhang, in *38th International Conference of Infrared Millimeter THz Waves, Mainz on the Rhine, Germany*, 1–6 September 2013, MO10-3.
[5]T. Rzesnicki, G. Gantenbein, S. Illy, J. Jelonnek, J. Jin, I. Gr. Pagonakis, B. Piosczyk, A. Schlaich, and M. Thumm, in *38th International Conference of Infrared Millimeter THz Waves, Mainz on the Rhine, Germany*, September 1–6, 2013, WE5-3.
[6]A. Malygin, S. Illy, I. Pagonakis, B. Piosczyk, S. Kern, J. Weggen, M. Thumm, J. Jelonnek, K. Avramides, L. Ives, D. Marsden, and G. Collins, IEEE Trans. Plasma Sci. **41**(10), 2717 (2013).
[7]O. Dumbrajs, *COAXIAL* (Helsinki University of Technology, 2001).
[8]K. A. Avramides, I. G. Pagonakis, C. T. Iatrou, and J. L. Vomvoridis, in *17th Joint Workshop on Electron Cyclotron Emission and Electron Cyclotron Resonance Heating, Deurne, The Netherlands, 7–11 May 2012, EC-17* [EPJ Web Conf. 32, 04016 (2012)].
[9]O. Dumbrajs and G. S. Nusinovich, Phys. Plasmas **20**, 073105 (2013).
[10]T. Idehara, K. Shibutani, H. Nojima, M. Pereyaslavets, K. Yoshida, I. Ogawa, and T. Tatsukawa, Int. J. Infrared Millimeter Waves **19**(10), 1303, (1998).
[11]K. A. Avramidis, I. G. Pagonakis, Z. C. Ioannidis, and I. G. Tigelis, in *38th International Conference of Infrared Millimeter THz Waves, Mainz on the Rhine, Germany*, 1–6 September 2013, MOP1-34.
[12]N. A. Zavolskiy and G. S. Nusinovich, Sov. J. Commun. Technol. Electron. **36**, 117 (1991).
[13]M. I. Airila and O. Dumbrajs, IEEE Trans. Plasma Sci. **30**, 846 (2002).
[14]M. I. Airila, Phys. Plasmas **10**, 296 (2003).
[15]O. Dumbrajs and G. S. Nusinovich, Phys. Plasmas **12**, 053106 (2005).
[16]O. Dumbrajs, G. S. Nusinovich, and T. M. Antonsen, Jr., Phys. Plasmas **19**, 063103 (2012).